OPEN

Intravoxel Incoherent Motion Diffusion Weighted Magnetic Resonance Imaging for Differentiation Between Nasopharyngeal Carcinoma and Lymphoma at the Primary Site

Xiao-Ping Yu, MM,†‡ Jing Hou, MM,* Fei-Ping Li, MM,* Hui Wang, MD,‡ Ping-Sheng Hu, MM,* Feng Bi, MM,* and Wei Wang, MD†*

Objective: The aim of the study was to investigate the utility of intravoxel incoherent motion (IVIM) diffusion-weighted magnetic resonance imaging (DWI) for differentiating nasopharyngeal carcinoma (NPC) from lymphoma.
Methods: Intravoxel incoherent motion–based parameters including the apparent diffusion coefficient (ADC), pure diffusion coefficient (*D*), pseudodiffusion coefficient (*D**), perfusion fraction (*f*), and *fD** (the product of *D** and *f*) were retrospectively compared between 102 patients (82 with NPC, 20 with lymphoma) who received pretreatment IVIM DWI.
Results: Compared with lymphoma, NPC exhibited higher ADC, *D*, *D**, *fD** values ($P < 0.001$) and *f* value ($P = 0.047$). The optimal cutoff values (area under the curve, sensitivity, and specificity, respectively) for distinguishing the 2 tumors were as follows: ADC value of 0.761×10^{-3} mm^2/s (0.781, 93.90%, 55.00%); *D*, 0.66×10^{-3} mm^2/s (0.802, 54.88%, 100.00%); *D**, 7.89×10^{-3} mm^2/s (0.898, 82.93%, 85.00%); *f*, 0.29 (0.644, 41.46%, 95.00%); and *fD**, 1.99×10^{-3} mm^2/s (0.960, 85.37%, 100.00%).
Conclusions: Nasopharyngeal carcinoma exhibits different IVIM-based imaging features from lymphoma. Intravoxel incoherent motion DWI is useful for differentiating lymphoma from NPC.

Key Words: intravoxel incoherent motion, diffusion-weighted magnetic resonance imaging, nasopharyngeal carcinoma, nasopharyngeal lymphoma, sensitivity and specificity

(*J Comput Assist Tomogr* 2016;40: 413–418)

In Southeast Asia and China, nasopharyngeal carcinoma (NPC) and lymphoma are two of the most common types of malignant tumors affecting the nasopharynx. The 2 tumors differ significantly from each other in terms of their epidemiology, biological behavior, treatment management, and prognosis. Accurate diagnosis is essential to optimize an individual treatment regimen. Currently, noninvasive imaging techniques, particularly magnetic resonance imaging (MRI) and computed tomography (CT), are the main tools used for diagnosing nasopharyngeal tumors; biopsy is also performed but this method is invasive. Unfortunately, both conventional MRI and CT demonstrate poor diagnostic accuracy in differentiating between lymphoma and NPC, because the 2 tumors often share similar imaging characteristics on both plain scan and traditional enhancement scan after the intravenous administration of contrast agent.[1] This situation may be attributed to the fact that conventional MRI and CT provide little useful functional information about the tumors.

As a functional imaging technique, diffusion-weighted MRI (DWI) can measure the mobility of water molecule in tissues. In recent years, studies have investigated the utility of DWI for the differentiation of benign and malignant lesions in the head and neck and for differentiation between certain histological types of malignant tumors.[2–5] Previous studies found that DWI could achieve high efficacy for discrimination among NPC, lymphoma, and squamous cell carcinoma in the head and neck.[2] For example, Fong et al[2] reported that NPC had a significantly higher apparent diffusion coefficient (ADC) value than lymphoma. However, conflicting result was reported in another study in which NPC and lymphoma presented similar ADC values.[5] It is well-known that the diffusion of water molecule in biological tissues is affected by both Brownian motion (pure diffusion) and microcirculatory perfusion (perfusion-related diffusion or pseudodiffusion). Based on a monoexponential model, traditional DWI calculates the total diffusion value and cannot distinguish between the 2 types of diffusion. It has been confirmed that microcirculation of the blood or perfusion in capillary networks can substantially affect the measurements of ADC value.[6] Therefore, traditional DWI is too simplistic to account for the complex motion of diffusion in tissues, because it does not take into account the blood perfusion in tumor tissues.

Intravoxel incoherent motion (IVIM) DWI, a new DWI technique, has the ability to separately quantitate the diffusion and perfusion effects.[6,7] Furthermore, blood perfusion can serve as an important biomarker for differentiating NPC from benign nasopharyngeal wall thickening.[8] Therefore, IVIM DWI is expected to be more accurate and sensitive than conventional DWI for characterizing nasopharyngeal lesions. A previous study indicated that the IVIM-based parameters for NPC differed from those for other squamous cell carcinomas in the head and neck.[9] However, to the best of our knowledge, few published studies have evaluated the feasibility of using IVIM DWI to differentiate between the most common malignancies (NPC and lymphoma) in the nasopharynx. We hypothesized that there are differences in the IVIM-based

From the *Department of Diagnostic Radiology, Hunan Cancer Hospital, the Affiliated Cancer Hospital of Xiangya School of Medicine, Central South University; †Department of Radiology, the Third Xiangya Hospital, Central South University; and ‡Hunan Provincial Key Laboratory of Translational Radiation Oncology, Hunan Cancer Hospital, Changsha, Hunan, PR China.
Received for publication October 23, 2015; accepted December 16, 2015.
Correspondence to: Wang Wei, MD, 138 Tongzipo Rd, Yuelu District, Changsha, 410013, Hunan, China (e-mail: cjr.wangwei@vip.163.com).
Supported by funding from the Affiliated Cancer Hospital of Xiangya School of Medicine, Central South University, Hunan, China (Project Number A2012-01). It was also supported by the National Key Clinical Specialty (Oncology Department) Development Program from National Health and Family Planning Commission of the PR China.
We haven't received funding from the following organizations: National Institutes of Health, Wellcome Trust, and Howard Hughes Medical Institute.
The authors declare no conflict of interest.

DOI: 10.1097/RCT.0000000000000391

parameters between NPC and lymphoma, and thus, IVIM DWI will be helpful for distinguishing between these 2 malignancies. To address this hypothesis, we compared the IVIM-based parameters of the 2 nasopharyngeal lesions at the primary site and evaluated the efficacy of IVIM-based parameters for differentiation between lymphoma and carcinomas in the nasopharynx.

MATERIALS AND METHODS

Patient Selection

This retrospective study was approved by the medical ethics committee of our institution and informed consent was obtained from all patients. We retrospectively analyzed the data of patients with newly diagnosed, pathologically confirmed nasopharyngeal lymphoma or NPC at our hospital from December 2014 to April 2015. The main inclusion criterion was that the patients had successfully undergone conventional MRI and IVIM DWI of the nasopharynx before treatment. The main exclusion criteria were as follows: (1) obvious motion or susceptibility artifacts around the skull base and paranasal sinuses on IVIM DWI images, which could prevent the IVIM analysis, or (2) difficulty in performing IVIM analysis because of a small tumor volume, which leads to poor signal-to-noise on DWI images. In total, 102 patients including 82 with NPC (80 nonkeratinizing, 2 keratinizing) and 20 with lymphoma (15 B-cell non-Hodgkin, 5 T-cell non-Hodgkin) were enrolled in the present study. The mean (SD) tumor volumes for lymphoma and NPC were 11.884(13.610)and 9.795(10.772) cm^3, respectively. For patients with NPC, the distribution of the T staging according to the 7th edition of the *American Joint Committee on Cancer* was as follows: T1, n = 8 (9.8%); T2, n = 29 (35.3%); T3, n = 19 (23.2%); and T4; n = 26 (31.7%).

Conventional MRI Protocol

All MRI examinations were performed on a 1.5-Tesla MRI scanner (Optima MR360; GE Healthcare, NJ) using a head and neck coil. The imaging protocol included axial T1-weighted spin-echo images (repetition time [TR]/echo time [TE], 580/7.8 milliseconds; slice number, 36; 5-mm slice thickness, 1-mm slice gap, number of excitations [NEXs], 2) and axial T2-weighted spin-echo images with fat suppression (TR/TE, 6289/85 milliseconds; slice number, 36; 5-mm section thickness, 1-mm intersection gap; NEX, 2). In addition, for contrast-enhanced axial and coronal T1-weighted spin-echo image acquisition, the contrast agent gadodiamide (Omniscan; GE Healthcare) was administrated intravenously at a dose of 0.1 mmol/kg of body weight.

Intravoxel Incoherent Motion DWI Protocol

The IVIM DWI was performed before the administration of gadodiamide. Ten *b* values (0, 50, 80, 100, 150, 200, 400, 600, 800 and 1000 s/mm^2) were applied with a single-shot diffusion-weighted spin-echo echo-planar or SS-SE-DW-EPI sequence. The lookup table of gradient directions was modified to allow multiple *b* value measurements in 1 series. Parallel imaging was used with an acceleration factor of 2. A local shim box covering the nasopharyngeal region was applied to minimize susceptibility artifacts. In total, 12 axial slices covering the nasopharynx were obtained with a 22-cm field of view, 5-mm slice thickness, 1-mm slice gap, TR of 4225 milliseconds, TE of 106 milliseconds, 128 × 130 matrix, and 4 NEX for all *b* values.

Intravoxel Incoherent Motion Analysis

All IVIM DWI data were transferred to an Advantage Workstation with Functool software (Version AW 4.6; GE Medical Systems) for postprocessing. Intravoxel incoherent motion analysis was performed using Cinetool Kit, a software package for multiple ADC measurements in the Functool software package, and fitted on a pixel-by-pixel basis according to the Levenberg-Marquardt algorithm.[10] Briefly, the major procedures of the IVIM analysis were as follows.

According to the IVIM theory described by Le Bihan and Turner,[11] the signal intensities and *b* values are related as follows:

$$S_b/S_0 = (1-f)\exp(-bD) + f\exp(-bD^*) \quad (1)$$

where S_b is the signal intensity with diffusion gradient b; S_0 is the signal intensity for a *b* value of 0 s/mm^2; *D* is the true diffusion coefficient (square millimeter per second) indicating the pure diffusion of water molecular; *f* is the microvascular volume fraction, representing the fraction of diffusion related to microcirculation perfusion; and *D** is the pseudodiffusion coefficient (square millimeter per second) caused by microcirculation perfusion. Because *D** is roughly 1 order of magnitude greater than D[12] − *bD** would be less than −3 at a high *b* value (>200 s/mm^2), and the term $f\exp(-bD^*)$ would be less than 0.05 *f*. In this case, the contribution of *D** to the signal ratio S_b/S_0 can be neglected, and Equation 1 was simplified as Equation 2 for an estimation of *D*:

$$S_b/S_0 = \exp(-bD) \quad (2)$$

Hence, for high *b* values (400, 600, 800, and 1000 s/mm^2), S_b was first fitted to Equation 2 using a linear model, and *D* was calculated. Secondly, fixing *D* at the value estimated previously and considering measurements from all 9 *b* values, *D** and *f* were determined from Equation 1 by a nonlinear Levenberg-Marquardt method.[10] Finally, the ADC was calculated from the traditional ADC equation, Equation 3, using data at *b* values of 0, 200, 400, 600, 800, and 1000 s/mm^2.

$$S_b/S_0 = \exp(-bADC) \quad (3)$$

Intravoxel incoherent motion analysis was independently and double-blindly performed by 2 observers (H.J and L.F, each with 10 years of experience in head and neck radiology) who were blinded to the pathological results of all nasopharyngeal lesions. First, the axial image section showing the primary tumor at its widest cross-section was firstly determined by using DWI (*b* = 800 s/mm^2), T2-weighted and contrast-enhanced T1-weighted images as references. Then, 3 regions of interest (ROIs) were manually drawn by each observer for each tumor on axial T2-weighted images at its widest section plus adjacent up and down sections, covering as much of the nasopharyngeal tumor as possible while avoiding the areas of necrosis, air, large vessels, and adjacent anatomical structures (ie, fat, muscle, bone) and then subsequently coregistered to IVIM DWI images for further analysis. Each IVIM-based metric value was acquired by each observer, and correspondingly 2 initial data points were generated, each of which was the average of the values obtained from the 3 ROIs by 1 observer. The eventual metric value for each tumor was the mean value of the 2 initial data points.

Statistical Analysis

The values of the IVIM-based parameters for each tumor type are expressed as mean(SD). A flow-related parameter was calculated from the product of *f* and *D**, denoted as *fD**.[11] The Mann-Whitney *U* test was used to compare the values of the IVIM-based parameters between the NPC and lymphoma groups. Receiver operating characteristic (ROC) curves were generated with respective cutoff values determined to accommodate best diagnostic accuracy according to the Youden Index. All statistical

TABLE 1. Comparing the IVIM-Based Parameter Values Between NPC and Lymphoma Using the Mann-Whitney *U* test

Groups	n	ADC ($\times 10^{-3}$ mm^2/s)	*D* ($\times 10^{-3}$ mm^2/s)	*D** ($\times 10^{-3}$ mm^2/s)	*f*	*fD** ($\times 10^{-3}$ mm^2/s)
NPC	82	0.981 (0.184)	0.726 (0.187)	17.901 (12.908)	0.280 (0.086)	4.975 (4.211)
Lymphoma	20	0.760 (0.1820)	0.534 (0.112)	5.885 (2.647)	0.233 (0.063)	1.237 (0.339)
P		<0.001	<0.001	<0.001	0.047	<0.001

analyses were performed using SPSS v19.0 software (SPSS Inc, Chicago, Ill). A *P* value of less than 0.05 was considered statistically significant.

RESULTS

The values of the IVIM-based parameters for NPC and lymphoma are summarized in Table 1. Figures 1 and 2 show representative images of NPC and lymphoma, respectively. From the ROC curve analysis, the respective optimal cutoff values of the IVIM-based parameters (with their respective area under the curve (AUC), sensitivity, and specificity) are shown in Table 2 and Figure 3. For differentiation, *fD** had the highest AUC (0.960), *D* and *fD** had the highest specificity (100%), whereas ADC had the highest sensitivity (93.90%).

DISCUSSION

Our data showed that NPC and lymphoma had distinctive IVIM-based diffusion and perfusion characteristics, suggesting that IVIM DWI may be potentially useful for detecting the tissue characteristics of nasopharyngeal tumors and differentiating NPC from lymphoma. In our study, NPC had a higher ADC value than lymphoma, which was similar to an earlier study by Fong et al[2] but different from a report by Ichikawa et al.[5] In the study,[5] the ADC value of nasopharyngeal lymphoma ([0.528{0.094} $\times$ 10^{-3} mm^2/s) was slightly lower than that of NPC ([0.567{0.057} $\times$ 10^{-3} mm^2/s), but the difference lacked statistical significance. This might be because of the small number of nasopharyngeal cases (8 NPCs and 7 lymphomas) enrolled in the study. Apparent diffusion coefficient, a combination of *D* and *D**, reflects the total diffusion within the tissue, including the pure diffusion and the perfusion-related diffusion of water molecular. Therefore, lymphoma exhibited a lower ADC value than NPC in our study, suggesting a lower level of pure diffusion and/or perfusion-related diffusion in lymphoma. For ADC, a cutoff value of 0.761 $\times$ 10^{-3} mm^2/s allows for differentiation between the 2 groups with a moderate AUC value of 0.781, a high sensitivity of 93.90%, and a low specificity of 55.00%, making it an useful imaging marker, which will require further improvement in its diagnostic efficacy.

Corresponding to the pure motion of water molecular, *D* depends mainly on the cell density and the composition of the extracellular matrix.[2,13] *D* is generally believed to be inversely correlated with the tissue cellularity and the nuclear-to-cytoplasm ratio.[14] Therefore, a reduced cellularity or low nuclear-to-cytoplasm ratio may result in an increased diffusivity of water molecular.[15] In addition, necrosis and cystic changes in tissues may also lead to an increase of the diffusivity.[16] In the present study, the significant difference in *D* value between NPC and lymphoma might result from differences in the microstructure between the 2 tumors. Compared with NPC, lymphoma is believed to be composed of condensed tumor cells with little cytoplasm, scarce amounts of stroma and necrosis. These differences in histological structure probably account for the lower *D* and ADC values observed in lymphoma compared with NPC. For *D*, a cutoff value of 0.660 $\times$ 10^{-3} mm^2/s could discriminate the 2 tumors with a moderate AUC value of 0.802 and a low sensitivity of 54.88% but with a very high specificity of 100.00%, suggesting that *D* may serve as an important imaging marker and that tumoral cellularity may be a key histological characteristic for differentiation between NPC and lymphoma.

According to the IVIM theory, *D** is proportional to the average blood velocity and the mean capillary segment length,[11] which indicates that *D** is linked to vascularity and perfusion in tissues. *D** depends on the microvessel attenuation of tissues.[17] It is well-known that NPC usually presents abundant vessels and hyperperfusion.[13,15] By contrast, lymphoma is always associated with poor perfusion,[18–20] compared with squamous cell carcinomas in the head and neck. A previous study confirmed that lymphoma showed significantly lower perfusion than NPC.[20] In our study, lymphoma presented a much lower *D** value than NPC, indicating that there is lower tumoral vascularity and perfusion in lymphoma than in NPC. To differentiate the 2 tumors, the optimal cutoff value for *D** was 7.89 $\times$ 10^{-3} mm^2/s, with a moderate sensitivity of 82.93%, a moderate specificity of 85.00%, and the second highest AUC of 0.898 among all the IVIM-based parameters, demonstrating that *D** is a potentially valuable predictor for differentiation.

Apart from *D**, *f* is another perfusion-related IVIM-based parameter corresponding to the fractional volume (percent) of capillary blood flowing in each voxel. Specifically, *f* is the ratio of the volume occupied by the MRI-detectable water in the capillary networks.[11] It seems theoretically possible that *f* is positively associated with perfusion. In fact, *f* was found to correlate well with microvessel density and perfusion parameters.[17,21] However, paradoxical findings of *f* have been recorded in several other tumors including NPC,[13] lung cancer, and prostate cancer.[22,23] Our data showed that NPC had a higher *f* value than lymphoma,

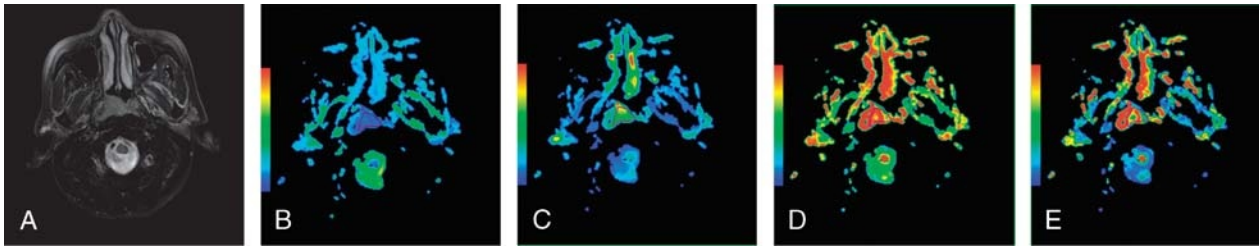

FIGURE 1. Representative images of NPC. Images 1A to 1E are axial T2-weighted images, ADC, *D*, *D**, and *f* maps, respectively. The ADC, *D*, *D**, and *f* values of the lesion were 0.890 $\times$ 10^{-3}, 0.669 $\times$ 10^{-3}, 13.426 $\times$ 10^{-3} mm^2/s, and 0.153, respectively.

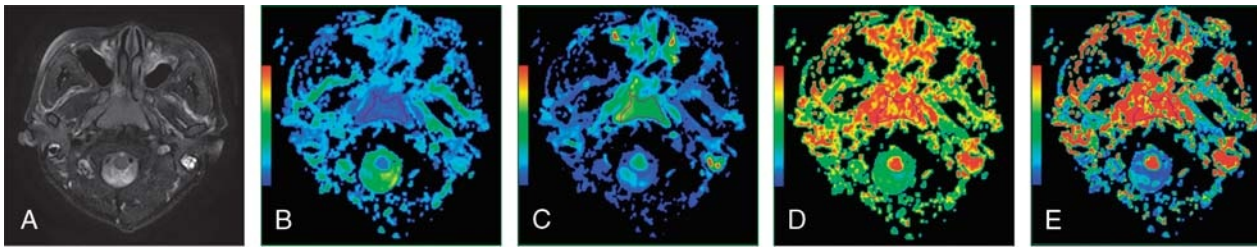

FIGURE 2. Representative images of a lymphoma. Images 2A to 2E are axial T2-weighted images, ADC, *D*, *D**, and *f* maps, respectively. The ADC, *D*, *D** and *f* values of the lesion were 0.734×10^{-3}, 0.545×10^{-3}, and 5.925×10^{-3} mm^2/s, and 0.149, respectively.

but the difference in *f* value between the 2 tumors was far less significant than those in the other IVIM-based parameters. In our study, the difference in *f* value between NPC and lymphoma was slight and just reached a statistical significance, which disagrees with the observation that NPC always exhibits more evident hyperperfusion than lymphoma.[20] The possible reasons for these conflicting results might be related to the MRI protocols and tissue characteristics under a magnetic field, which need to be verified in further studies. For example, the measurement of *f* was found to be greatly dependent on the TE and the T2 relaxation time.[24] During IVIM DWI, a longer TE would cause a greater signal decay at low *b* values, and consequently, the *f* value would increase. This TE dependence effect would probably be significant for IVIM DWI on organs exhibiting short T2 time similar to blood, such as NPC and lymphoma. In a previous IVIM DWI study on the nasopharynx using a relatively long TE of 58 milliseconds, the *f* value for NPC was significantly lower than that for enlarged adenoids,[13] inconsistent with the increased perfusion, which is commonly associated with malignant tumors such as NPC. In addition, a longer T2 time for the tissue will result in a lower measured value of *f*.[25] The T2 time was thought to vary greatly among different tumors.[26] Indeed, NPC and lymphoma always demonstrated different T2 time. However, to our knowledge, few published studies have described the exact T2 time for NPC or lymphoma. Wang et al[27] found that small foci of necrosis and cystic change were confirmed by pathologic examination but were not detected on MRI images in head and neck tumors. Simultaneously, it is well-known that necrosis and cystic changes are more common in NPC than in lymphoma. Therefore, we propose that the T2 time for NPC might be longer than that for lymphoma, leading to a smaller difference in *f* value between NPC and lymphoma. This may be similar to the suggestion by Wang et al[22] that a higher *f* value in obstructive pulmonary consolidation than in lung cancer might be due to exudation.

Another blood flow-related IVIM-based parameter, *fD**, is equal to the product of *f* and *D**. In brain, *fD** was suggested to be directly proportional to the cerebral blood flow, and it could be used to estimate the relative perfusion or blood flow in tissues.[6,21,28,29] Parameter *fD** is believed to depend on the relationships among the microvascular anatomy, the vascular permeability, and the blood flow dynamics.[21] Lee et al[21] found a moderate positive correlation between *fD** value and dynamic contrast enhancement MRI parameters in cervical cancers. Federau et al[29] demonstrated that the *fD** value for the visual cortex and white matter increased during visual stimulation. In another study by Federau et al,[30] *D** and *fD** values were significantly larger during systole than during diastole, whereas *D* and *f* values were not obviously altered in the brain of healthy human. In our study, there was a prominent difference in *fD** value between NPC and lymphoma, indicating that the 2 tumors differ markedly from each other in their microcirculatory anatomy and function. Based on the ROC analysis, the optimal cutoff value for *fD** was 1.99×10^{-3} mm^2/s, with a moderate sensitivity of 85.37% and a very high specificity of 100.00% for differentiation. Furthermore, *fD** had the largest AUC value of 0.960 among all the IVIM-based parameters, with a 95% confidence interval (CI) from 0.902 to 0.989, and it did not overlap with any other IVIM-based parameter, revealing that it might be a potentially valuable predictor for differentiation between NPC and lymphoma. Unfortunately, *fD** and *D** had the largest SDs among the 5 IVIM-based parameters evaluated in our study, which would severely limit their clinical application. The large standard deviation of *D** indicates a poor reproducibility associated with the measurement of parameter *D**, which has been widely reported.[29,31] Possible reasons for this poor reproducibility include the distortion of DWI, pulsation artifacts from the heart or great vessels without electrocardiograph gating, noisy *D** map, and microvessel density scores that also often show large variations across the tumors.[17] Therefore, the image quality and signal-to-noise ratio for *fD** and *D** on IVIM DWI should be improved to make the 2 parameters more reliable.

Our study has several limitations. First, the patient cohort for lymphoma was relatively small. Second, we did not correlate the IVIM-based parameters with histological features, such as tumor cell density, nuclear-to-cytoplasm ratio, and microvessel density. However, the pathological diagnosis of nasopharyngeal tumors is usually based on biopsy specimens, which are always small and obtained from the surface of the lesions. It is well-known that malignant tumors often exhibit histological heterogeneity, namely, the surface region of a tumor is always associated with greater vascularity and less necrosis on a microscopic level in comparison of the central area. Therefore, the pathological features of biopsy specimens may not comprehensively reflect those of the entire

TABLE 2. Optimal Cutoff Values for Differentiation Between NPC and Lymphoma Based on ROC Curve Analysis

Parameters	AUC (95% CI)	Cutoff Value	Sensitivity (95% CI), %	Specificity (95% CI), %	Youden Index (95% CI)
ADC	0.781 (0.688–0.857)	0.761×10^{-3} mm^2/s	93.90 (86.3–98.0)	55.00 (31.5–76.9)	0.489 (0.688–0.857)
D	0.802 (0.711–0.874)	0.66×10^{-3} mm^2/s	54.88 (43.5–65.9)	100.00 (83.2–100.0)	0.549 (0.405–0.634)
*D**	0.898 (0.711–0.874)	7.89×10^{-3} mm^2/s	82.93 (73.0–90.3)	85.00 (62.1–96.8)	0.679 (0.522–0.792)
f	0.644 (0.543–0.736)	0.29	41.46 (30.7–52.9)	95.00 (75.1–99.9)	0.365 (0.210–0.476)
*fD**	0.960 (0.902–0.989)	1.99×10^{-3} mm^2/s	85.37 (75.8–92.2)	100.00 (83.2–100.0)	0.854 (0.730–0.915)

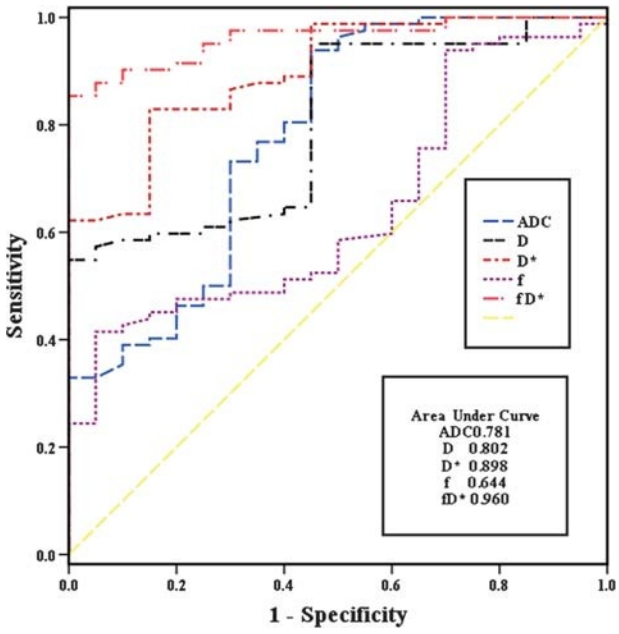

FIGURE 3. Receiver operating characteristic curves for the IVIM-based parameter values with their respective areas under the curves.

tumor. Thirdly, the IVIM analysis in our study was based on drawing an ROI covering the entire solid parenchyma of the tumors to survey the mean value. This does not adequately reflect the heterogeneity of tumors such as NPC. Nevertheless, the information gathered from the entire tumor might be more readily applicable to tumor evaluation.[32–34] Our IVIM analysis excluded grossly visible necrosis in tumors, whereas cystic or necrotic portions of tumors might significantly affect the measurements of IVIM-based parameters.[35] Further studies using regional hot-spot analysis, intratumor pixel-by-pixel analysis, and analysis of the cystic or necrotic portions might be meaningful for comprehensively characterizing different tumors.

In conclusion, our preliminary study shows that NPC exhibits different IVIM-based imaging features from lymphoma. Intravoxel incoherent motion DWI is potentially useful for differentiation between the 2 nasopharyngeal tumors, which often present a clinical diagnostic dilemma. Considering that *fD** and *D** are usually more variable, *D* may be more reliable and useful in clinical practice.

REFERENCES

1. Vogl T, Dresel S, Schedel H, et al. MRI of the nasopharynx with Gd-DTPA: its value and differential diagnostic criteria. *Rofo*. 1989;150:516–522.
2. Fong D, Bhatia KS, Yeung D, et al. Diagnostic accuracy of diffusion-weighted MR imaging for nasopharyngeal carcinoma, head and neck lymphoma and squamous cell carcinoma at the primary site. *Oral Oncol*. 2010;46:603–606.
3. Maeda M, Kato H, Sakuma H, et al. Usefulness of the apparent diffusion coefficient in line scan diffusion-weighted imaging for distinguishing between squamous cell carcinomas and malignant lymphomas of the head and neck. *AJNR Am J Neuroradiol*. 2005;26:1186–1192.
4. Kato H, Kanematsu M, Kawaguchi S, et al. Evaluation of imaging findings differentiating extranodal non-Hodgkin's lymphoma from squamous cell carcinoma in naso- and oropharynx. *Clin Imaging*. 2013;37:657–663.
5. Ichikawa Y, Sumi M, Sasaki M, et al. Efficacy of diffusion-weighted imaging for the differentiation between lymphomas and carcinomas of the nasopharynx and oropharynx: correlations of apparent diffusion coefficients and histologic features. *AJNR Am J Neuroradiol*. 2012;33:761–766.
6. Le Bihan D, Breton E, Lallemand D, et al. Separation of diffusion and perfusion in intravoxel incoherent motion MR imaging. *Radiology*. 1988; 168:497–505.
7. Patel J, Sigmund EE, Rusinek H, et al. Diagnosis of cirrhosis with intravoxel incoherent motion diffusion MRI and dynamic contrast-enhanced MRI alone and in combination: preliminary experience. *J Magn Reson Imaging*. 2010;31:589–600.
8. Jin G, Su D, Liu L, et al. The accuracy of computed tomographic perfusion in detecting recurrent nasopharyngeal carcinoma after radiation therapy. *J Comput Assist Tomogr*. 2011;35:26–30.
9. Marzi S, Piludu F, Vidiri A. Assessment of diffusion parameters by intravoxel incoherent motion MRI in head and neck squamous cell carcinoma. *NMR Biomed*. 2013;26:1806–1814.
10. Marquardt D. An algorithm for least-squares estimation of nonlinear parameters. *SIAM J Appl Math*. 1963;11:431–441.
11. Le Bihan D, Turner R. The capillary network: a link between IVIM and classical perfusion. *Magn Reson Med*. 1992;27:171–178.
12. Le Bihan D. Intravoxel incoherent motion perfusion MR imaging: a wake-up call. *Radiology*. 2008;249:748–752.
13. Zhang SX, Jia QJ, Zhang ZP, et al. Intravoxel incoherent motion MRI: emerging applications for nasopharyngeal carcinoma at the primary site. *Eur Radiol*. 2014;24:1998–2004.
14. Jenkinson MD, du Plessis DG, Smith TS, et al. Cellularity and apparent diffusion coefficient in oligodendroglial tumors characterized by genotype. *J Neurooncol*. 2010;96:385–392.
15. White ML, Zhang Y, Robinson RA. Evaluating tumors and tumor like lesions of the nasal cavity, the paranasal sinuses, and the adjacent skull base with diffusion-weighted MRI. *J Comput Assist Tomogr*. 2006;30:490–495.
16. Sumi M, Ichikawa Y, Nakamura T. Diagnostic ability of apparent diffusion coefficients for lymphomas and carcinomas in the pharynx. *Eur Radiol*. 2007;17:2631–2637.
17. Lee HJ, Rha SY, Chung YE, et al. Tumor perfusion-related parameter of diffusion-weighted magnetic resonance imaging: correlation with histological microvessel density. *Magn Reson Med*. 2014;71:1554–1558.
18. Kitamoto E, Chikui T, Kawano S, et al. The application of dynamic contrast-enhanced MRI and diffusion-weighted MRI in patients with maxillofacial tumors. *Acad Radiol*. 2015;22:210–216.
19. Matsuzaki H, Hara M, Yanagi Y, et al. Magnetic resonance imaging (MRI) and dynamic MRI evaluation of extranodal non-Hodgkin lymphoma in oral and maxillofacial regions. *Oral Surg Oral Med Oral Pathol Oral Radiol* 2012 ;113:126–133.
20. Lee FK, King AD, Ma BB, et al. Dynamic contrast enhancement magnetic resonance imaging (DCE-MRI) for differential diagnosis in head and neck cancers. *Eur J Radiol*. 2012;81:784–788.
21. Lee EY, Hui ES, Chan KK, et al. Relationship between intravoxel incoherent motion diffusion-weighted MRI and dynamic contrast-enhanced MRI in tissue perfusion of cervical cancers. *J Magn Reson Imaging*. 2015;42:454–459.
22. Wang LL, Lin J, Liu K, et al. Intravoxel incoherent motion diffusion-weighted MR imaging in differentiation of lung cancer from obstructive lung consolidation: comparison and correlation with pharmacokinetic analysis from dynamic contrast-enhanced MR imaging. *Eur Radiol*. 2014;24:1914–1922.
23. Shinmoto H, Oshio K, Tanimoto A, et al. Biexponential apparent diffusion coefficients in prostate cancer. *Magn Reson Imaging*. 2009;27:355–359.
24. Lemke A, Laun FB, Simon D, et al. An in vivo verification of the intravoxel incoherent motion effect in diffusion-weighted imaging of the abdomen. *Magn Reson Med* 2010 ;64:1580–1585.
25. Sumi M, Van Cauteren M, Sumi T, et al. Salivary gland tumors: use of intravoxelincoherent motion MR imaging for assessment of diffusion and

perfusion for the differentiation of benign from malignant tumors. *Radiology*. 2012;263:770–777.

26. Clark CA, Le Bihan D. Water diffusion compartmentation and anisotropy at high b values in the human brain. *Magn Reson Med*. 2000;44:852–859.
27. Wang J, Takashima S, Takayama F, et al. Head and neck lesions: characterization with diffusion-weighted echo-planar MR imaging. *Radiology*. 2001;220:621–630.
28. Wirestam R, Borg M, Brockstedt S, et al. Perfusion-related parameters in intravoxel incoherent motion MR imaging compared with CBV and CBF measured by dynamic susceptibility-contrast MR technique. *Acta Radiol*. 2001;42:123–128.
29. Federau C, O'Brien K, Birbaumer A, et al. Functional mapping of the human visual cortex with intravoxel incoherent motion MRI. *PLoS One*. 2015;10:e0117706.
30. Federau C, Hagmann P, Maeder P, et al. Dependence of brain intravoxel incoherent motion perfusion parameters on the cardiac cycle. In: *PLoS One*. 2013;8:e72856.
31. Dyvorne HA, Galea N, Nevers T, et al. Diffusion-weighted imaging of the liver with multiple b values: effect of diffusion gradient polarity and breathing acquisition on image quality and intravoxel incoherent motion parameters-a pilot study. *Radiology*. 2013;266: 920–929.
32. Moffat BA, Chenevert TL, Meyer CR, et al. The functional diffusion map: an imaging biomarker for the early prediction of cancer treatment outcome. *Neoplasia*. 2006;8:259–267.
33. Ungersma SE, Pacheco G, Ho C, et al. Vessel imaging with viable tumor analysis for quantification of tumor angiogenesis. *Magn Reson Med*. 2011; 65:889–899.
34. Kim JH, Im GH, Yang J, et al. Quantitative dynamic contrast-enhanced MRI for mouse models using automatic detection of the arterial input function. *NMR Biomed*. 2012;25:674–684.
35. Maeda M, Kawamura Y, Tamagawa Y, et al. Intravoxel incoherent motion (IVIM) MRI in intracranial, extraaxial tumors and cysts. *J Comput Assist Tomogr*. 1992;16:514–518.